applied sciences

MDPI

Article

Experiment Investigation of Bistable Vibration Energy Harvesting with Random Wave Environment

Qiong Wu [1,*], Hairui Zhang [1,*], Jie Lian [2,*], Wei Zhao [3,*], Shijie Zhou [4,*] and Xilu Zhao [4,*]

[1] College of Mechatronic Engineering, Nanjing Forestry University, Nanjing 210037, China
[2] Sangyo Shinkou Co., Ltd., Aichi 476-0001, Japan
[3] Weichai Global Axis Technology Co., Ltd., Minami-Aoyama, Tokyo 107-0062, Japan
[4] Saitama Institute of Technology, Fukaya 369-0293, Japan
* Correspondence: wuqiong@njfu.edu.cn (Q.W.); zhanghairui@njfu.edu.cn (H.Z.); renketu0724@gmail.com (J.L.); shunsuke0390@icloud.com (W.Z.); zsj847497659@gmail.com (S.Z.); zhaoxilu@sit.ac.jp (X.Z.)

Abstract: The energy harvested from the renewable energy has been attracting a great potential as a source of electricity for many years; however, several challenges still exist limiting output performance, such as the package and low frequency of the wave. Here, this paper proposed a bistable vibration system for harvesting low-frequency renewable energy, the bistable vibration model consisting of an inverted cantilever beam with a mass block at the tip in a random wave environment and also develop a vibration energy harvesting system with a piezoelectric element attached to the surface of a cantilever beam. The experiment was carried out by simulating the random wave environment using the experimental equipment. The experiment result showed a mass block's response vibration was indeed changed from a single stable vibration to a bistable oscillation when a random wave signal and a periodic signal were co-excited. It was shown that stochastic resonance phenomena can be activated reliably using the proposed bistable motion system, and, correspondingly, large-scale bistable responses can be generated to realize effective amplitude enlargement after input signals are received. Furthermore, as an important design factor, the influence of periodic excitation signals on the large-scale bistable motion activity was carefully discussed, and a solid foundation was laid for further practical energy harvesting applications.

Keywords: bistable vibration; energy harvesting; stochastic resonance; random wave environment

check for updates

Citation: Wu, Q.; Zhang, H.; Lian, J.; Zhao, W.; Zhou, S.; Zhao, X. Experiment Investigation of Bistable Vibration Energy Harvesting with Random Wave Environment. *Appl. Sci.* **2021**, *11*, 3868. https://doi.org/10.3390/app11093868

Academic Editor: Junhong Park

Received: 21 January 2021
Accepted: 13 April 2021
Published: 25 April 2021

1. Introduction

In the past, the research and development of renewable energy sources and other resource utilization is a very important research topic. Many researchers have studied the vibration power generation method in the natural environment and published many research results [1–6].

Among them, applying the stochastic resonance phenomenon as a possible way to utilize the rich energy contained in complex random waves effectively has attracted much attention. Stochastic resonance is a kind of physical phenomenon. By applying a weak periodic signal to a nonlinear system in a random noise environment, the response of the system is amplified under a certain probability. Stochastic resonance was first proposed by Benzi et al. in 1981 to verify the periodicity of the ice age [7]. After that, theoretical research on stochastic resonance has been carried out, and many research results have been published [8–11]. Stochastic resonance is applied to many new fields, and, in the field of measurement signal processing, the system that detects the weak input signal by using the noise resonance phenomenon by adding noise signal to measure the weak input signal is studied [12–15]. In the field of computer image processing, it is possible to process the dark image relatively easily by using the stochastic resonance system as an image sensor of the image to clear the dark image [16–19].

On the other hand, some studies have published the stochastic resonance phenomenon results in which periodic signals and noise signals are simultaneously inputted into nonlinear bistable systems to amplify the system response amplitude [20–23]. Among them, the most common case is to use the relative repulsive force between the permanent magnet installed at the front of the cantilever beam and the permanent magnet fixed near the cantilever beam to form the bistable vibration model [24–28]. In addition, the gravity of the mass installed in the front of the inverted cantilever beam is used to form the double stable vibration model [29–31].

With about, harvesting energy technology will also be used in other vibration fields. V.G. Cleante et al. [32] proposed as a potential energy source to power wireless sensors by track vibration, it was found that the 7th trainload frequency had the highest amplitude in four out of the five cases. Feng Qiang et al. [33] presented the design, modeling and experimental tests of a novel piezoelectric energy harvester with a two-stage force-amplification compliant mechanism for scavenging energy from human walking. Rodrigues C. et al. [34] proposed and critically assessed triboelectric nano generators (TENGs) as a promising technology for integration into wave buoys, which opens new horizons and strategies to apply TENGs in marine applications, considering realistic hydrodynamic behaviors of floating bodies. Y. S. Sheng et al. [35] proposed piezoelectric energy harvesting from wind-induced vibration, which is an attractive power solution for the micro electric devices in field work.

In order to realize the vibration power generation by using the stochastic resonance of the bistable vibration model, focusing on the vibration of the vehicle tire at low speed, the cantilever beam with a permanent magnet at the front end is installed on the wheel structure, and the random noise generated by the bump of the road surface and the periodicity generated by the rotation of the tire have been published. The research results show that, in the nonlinear bistable energy harmonic system using power as an input signal, from the practical point of view, the power generation device caused by stochastic resonance phenomenon is used as the self-power supply of tire air sensor [36,37]. However, in the field of renewable energy sources resources utilization, the research results of nonlinear bistable energy harmonic system in random wave environment have not been found by using stochastic resonance phenomenon.

In this paper, we propose a bistable vibration model consisting of an inverted cantilever beam with a mass block at the tip in a random wave environment and also develop a vibration energy harvesting system with a piezoelectric element attached to the surface of a cantilever beam. The water tank or vibration device is used to reproduce the stochastic resonance phenomenon under the random wave environment. The characteristics of the stochastic resonance phenomenon and the vibration power generation are discussed. The influence of the stochastic resonance phenomenon on the vibration energy collection system is verified by using the stochastic resonance phenomenon in the random wave environment, and the design range of the proposed bistable vibration model is also discussed. The predicted results of the vibration characteristics, potential energy distribution and excitation frequency of the proposed bistable vibration model are compared with the experimental results, and it seems to have advanced toward the practical development of the bistable vibration harvesting system from now on.

2. Materials

2.1. Bistable Vibration Harvesting System on the Random Wave

In order to generate the stochastic resonance phenomena, the existence of the random noise input signal, the periodic excitation force and the nonlinear bistable system are mentioned as three requirements. In this study, the experimental system of bistable vibration in the random wave environment shown in Figure 1 is devised.

As shown in Figure 1, the experimental system consists of three parts: a water tank, a random wave generator, and a bistable vibration model body. It is fixed to the bottom of the tank using an elastic plate under the vibration model body in the center of the water tank, and the vibration model body consists of a wooden box that floats halfway on the water surface. In the vibration model body, in order to cause the phenomenon of probabilistic resonance, a mini shaker with periodic exciting force is set up.

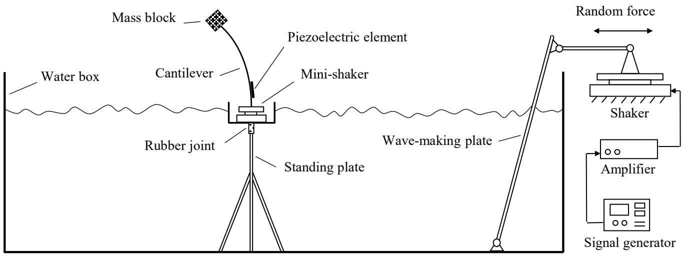

Figure 1. The diagram of experimental settings of bistable vibration power generation system in random wave environment.

In order to realize vibratory power generation, a piezoelectric element is stuck near the root of a cantilever beam, and the vibration generating voltage can be obtained from a piezoelectric element that is bent and deformed along with the vibration of the vibration model.

In order to generate a random exciting force by the waves, it is connected to the vibration model body and the elastic plate under the vibration model body by the rubber plate. On the other hand, in order to generate a random wave, a wave generator is installed on the left side of the water tank. It is fixed to the bottom of the water tank by the pin connecting element of the rotation free under the wave making plate. It is connected to the shaking table by the link mechanism on the wave-making board, and the amplifier and the signal generator are installed at the end of the shaking table.

In order to verify the amplification effect and the vibration generation performance by the stochastic resonance using the bistable vibration power generation system in the random wave environment shown in Figure 1, an experimental apparatus and a measuring system shown in Figure 2 were developed.

Figure 2. The experimental equipment and measurement system for bistable vibration power generation system in random wave environment.

The measurement system shown in Figure 2 is used, and the verification experiment is carried out according to the following procedure. Firstly, a random excitation signal is generated from the signal generator and sent to the amplifier, and the random excitation signal amplified by the amplifier is sent to the shaking table. The wave generator is vibrated by the shaking table, and random waves are generated on the surface of the water in the water tank. The stochastic resonance is generated in the vibration model by shaking the shaking table from the mini shaking table.

In addition, in order to measure the response vibration displacement of the vibration model in the center of the water tank and the voltage generated by the vibration generated by the piezoelectric element, the measurement marks are pasted on the mass block and support point, respectively. In the measurement, the measurement marker's motion locus is recorded using the high-speed camera, the tracking software is used, and the vibration displacement data of the mass block and support point can be produced. The output lead of the piezoelectric element is directly connected to the data logger to record the voltage signal of the oscillatory power generation using the data logger.

2.2. Bistable Vibration Characteristics

For the purpose of the examination, the cantilever beam and the concentrated mass block on the vibration model body shown in Figure 3 are separated from each other, and the other part of the vibration model body is fixed to the end of the analytical model. Noise-induced by random waves and periodic excitation force by a small shaker is applied to the fixed end.

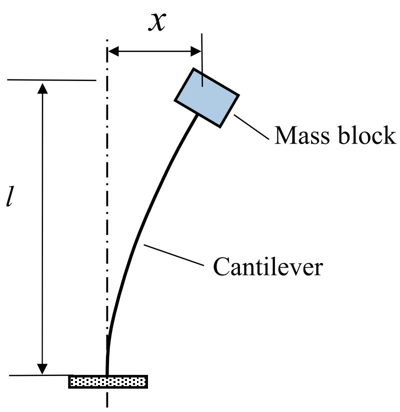

Figure 3. The bistable vibration model of a cantilever with a mass block at the tip.

In reference [29], a detailed theoretical analysis of an inverted cantilever beam with a mass block at the front end is carried out. Based on the research results, the motion equation of the motion model shown in Figure 3 is expressed as follows.

$$\begin{aligned}&\left[I_t N_5^2 + m + \rho A N_1 + \left(\rho A N_3 + m N_4^2 + I_t N_5^4\right)x^2\right]\ddot{x} + \left[\rho A N_3 + m N_4^2 + I_t N_5^4\right]x\dot{x}^2 \\ &\quad + \left[EIN_6 - \rho A g N_8 - m g N_4 + 2EIN_7 x^2\right]x = -[\rho A N_2 + m]\ddot{x}_t.\end{aligned} \tag{1}$$

However, m is the mass of the mass block, L is the length of the beam, E is the elastic Young's modulus of the beam, I is the secondary moment of the cross section of the beam, ρ is the density of the beam, A is the cross sectional area of the beam, g is the gravitational acceleration, and I_t is the rotational inertia moment of the mass block, $\ddot{x}_t$ is the accelerate. Symbols N_1~N_8 are represented by the following equations:

$$N_1 = \frac{(3\pi - 8)L}{2\pi}, \tag{2}$$

$$N_2 = \frac{(\pi - 2)L}{\pi}, \tag{3}$$

$$N_3 = \frac{\pi^2(2\pi^2 - 9)}{384L}, \quad (4)$$

$$N_4 = \frac{\pi^2}{8L}, \quad (5)$$

$$N_5 = \frac{\pi}{2L}, \quad (6)$$

$$N_6 = \frac{\pi^4}{32L^3}, \quad (7)$$

$$N_7 = \frac{\pi^6}{2^9 L^5}, \quad (8)$$

$$N_8 = \frac{\pi^2 - 4}{16}. \quad (9)$$

Equations (2) to (9) are substituted for the Equation (1), and the equations of motion are expressed as follows.

$$\left(M_1 + J_1 x^2\right)\ddot{x} + J_1 x \dot{x}^2 + \left(K_1 + J_2 x^2\right)x = -M_2 \ddot{x}_t. \quad (10)$$

Then,

$$M_1 = \frac{\pi^2}{4L^2} I_t + m + \rho A L \frac{(3\pi - 8)}{2\pi}, \quad (11)$$

$$J_1 = \rho A \frac{\pi^2(2\pi^2 - 9)}{384L} + m\frac{\pi^4}{64L^2} + \frac{\pi^4}{16L^4} I_t, \quad (12)$$

$$K_1 = EI\frac{\pi^4}{32L^3} + \rho A g \frac{\pi^2 - 4}{16} - mg\frac{\pi^2}{8L}, \quad (13)$$

$$J_2 = EI\frac{\pi^6}{2^8 L^5}, \quad (14)$$

$$M_2 = \rho A L \frac{\pi - 2}{\pi} + m. \quad (15)$$

From the equation of motion (10), the potential energy of the proposed vibration model is expressed by the following equation.

$$U = \frac{1}{2} EI\left(\frac{\pi^4}{32L^3}x^2 + \frac{\pi^6}{2^9 L^5}x^4\right) - \frac{1}{8}\left(\frac{\pi^2}{4} - 1\right)\rho A g x^2 - \frac{\pi^2}{16L} m g x^2. \quad (16)$$

As an actual structural parameter of the vibration model shown in Figure 1, the mass of the mass block is 0.15 kg, the length of the beam is 380 mm, the width is 30 mm, the thickness of the plate is 0.5 mm, the young's modulus of the beam material is 210 GPa, the density is 7850 kg/m^3, and the gravitational acceleration is 9.8 m/s^2, and the result of the potential energy distribution shown in Figure 4 is obtained.

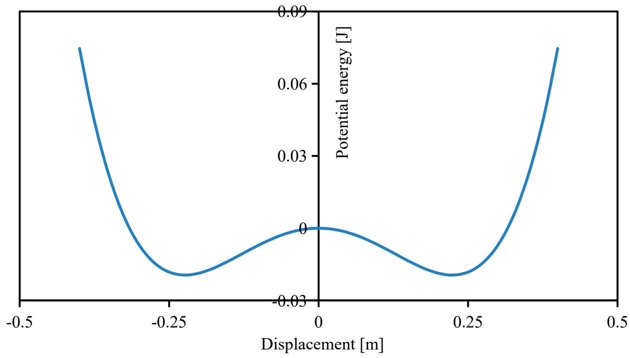

Figure 4. The potential energy distribution of bistable vibration model.

In Figure 4, the abscissa is the transverse displacement of the mass block, and the ordinate is the potential energy, it is found from the figure that the potential energy distribution has two-well characteristics (There is a valley of potential energy at each side of the graph, the valley bottom is the equilibrium position of the mass block at rest). At the center of the graph, there is a mountain potential energy peak, which corresponds to the potential energy at which the mass block passes the vibration model's central position.

In general, the mass receiving relatively weak random excitation signal vibrates singly on the left or right side, as shown in Figure 5a,b. In order to generate stochastic resonance, a periodic excitation signal is needed to be applied to the mass block to cross the central position and generate a bistable vibration state across both sides, as shown in Figure 5c. Therefore, the amplification effect of this kind of stochastic resonance can play a role in vibration power generation, which is helpful to improve the efficiency of traditional vibration power generation.

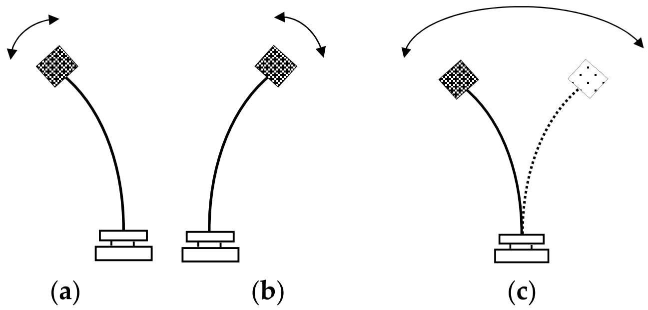

Figure 5. Three vibration states of the bistable vibration model. (**a**) The single stable vibration state on the left. (**b**) The single stable vibration state on the right. (**c**) The bistable vibration state.

The time series displacement signal simulating random waves used in the verification experiment of this research and the spectral distribution in the frequency domain is shown in Figure 6, and it is understood that the frequency components contained in the random signal are distributed relatively uniformly.

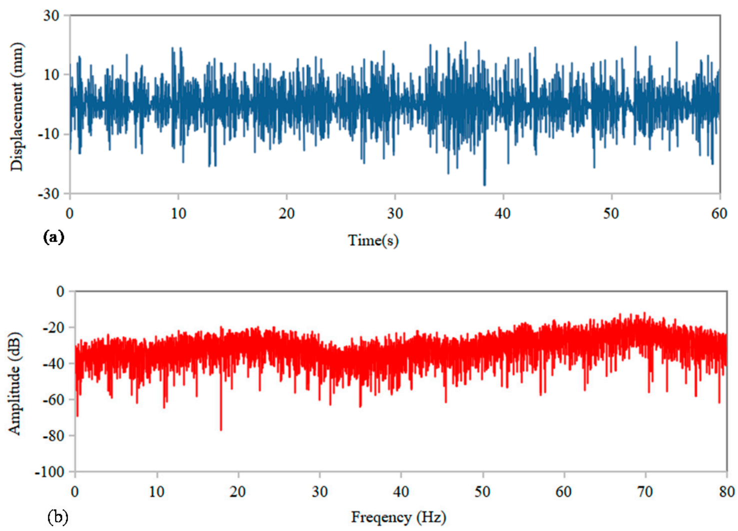

Figure 6. The time series displacement of random signal and its frequency component distribution. (**a**) Vibration displacement. (**b**) Power spectrum.

2.3. Prediction of Periodic Signals Subject to Stochastic Resonance

In order to generate the stochastic resonance, periodic signals with an appropriate frequency from outside are required. In Reference [8], a predictive equation is proposed for the frequency of periodic signals in which stochastic resonance is most likely to occur in the bistable oscillation model.

$$f_K = \frac{\omega_0 \omega_b}{4\pi q} \exp\left(-\frac{\Delta U}{mD}\right). \tag{17}$$

Here, ω_0 and ω_b are the natural angular frequencies of the stable point x_b and the unstable point x_0 on both sides of the potential energy of the bistable vibration model, respectively, q is the attenuation parameter, ΔU is the potential difference expressed by the difference between the maximum and minimum potential energy, and D is the random vibration intensity expressed by the white noise signal, which can be calculated according to the following equation, respectively.

$$\omega_0 = \sqrt{\frac{|U''(x_0)|}{m}}, \tag{18}$$

$$\omega_0 = \sqrt{\frac{|U''(x_b)|}{m}}, \tag{19}$$

$$\mathrm{q} = \frac{c}{m}, \tag{20}$$

$$\Delta U = U(x_0) - U(x_b), \tag{21}$$

$$D = \frac{1}{2N} \sum\nolimits_{i=0}^{N} \left(\dot{x}_i - \dot{x}_{aver}\right)^2. \tag{22}$$

Here, c is the attenuation coefficient, $\dot{x}_i$ and $\dot{x}_{aver}$ are the measured value and the average value of the velocity of the moving body when the random signal is used for excitation, respectively, and N is the sample point of the measurement experiment. When designing the bistable vibration model, the random vibration intensity D represented by Equation (22) can be measured firstly, which makes the ΔU represented by Equation (21) slightly larger than that of mean kinetic energy of random vibration mD. In the case of only random excitation, the mass block vibrates at a slightly larger amplitude on the left or right side of the central axis. When the periodic excitation signal is given, it is ensured that even the amplitude with a small periodicity can produce probability resonance.

The symmetry condition determines the position of the unstable point x_0 = 0 at the center of the potential energy. The position of the stable point x_b on both sides of the potential energy can be calculated by the following.

$$x_b = \pm\sqrt{\frac{\rho A g N_8 + m g N_4 - EIN_6}{2EIN_7}}. \tag{23}$$

Equations (5), (7)–(9) are substituted by Equation (23) to obtain the following equation,

$$x_b = \pm\sqrt{\frac{16\rho A g L^5(\pi^2 - 4) + 32\pi^2 m g L^4 - 8\pi^4 EIL^2}{\pi^6 EI}}. \tag{24}$$

The configuration parameter of the proposed bistable oscillation model is substituted for Equation (24) to obtain x_b = 0.2236m. The following equation is obtained by differentiating twice the potential energy Equation (16).

$$U'' = \frac{1}{2}EI\left(\frac{\pi^4}{16L^3} + \frac{\pi^6}{384L^5}x^2\right) - \frac{1}{4}\left(\frac{\pi^2}{4} - 1\right)\rho A g - \frac{\pi^2}{8L} m g, \tag{25}$$

The values x_0 and x_b are substituted into Equations (25), (18) and (19), respectively, and the respective angular frequencies are obtained as follows.

$$\omega_0 = \sqrt{\frac{1}{m}\left|\frac{\pi^4 EI}{32L^3} - \frac{\pi^2 - 4}{16}\rho Ag - \frac{\pi^2 mg}{8L}\right|} = 3.2200 \text{ rad/s}, \tag{26}$$

$$\omega_b = \sqrt{\frac{1}{m}\left|\frac{\pi^4 EI}{32L^3} + \frac{\pi^6 EI}{728L^5}x_b^2 - \frac{\pi^2 - 4}{16}\rho Ag - \frac{\pi^2 mg}{8L}\right|} = 2.6292 \text{ rad/s}. \tag{27}$$

The corresponding natural frequencies corresponding to them are as follows.

$$f_0 = \frac{\omega_0}{2\pi} = 0.5125 \text{ Hz}, \tag{28}$$

$$f_b = \frac{\omega_b}{2\pi} = 0.4185 \text{ Hz}. \tag{29}$$

According to the measured results of actual vibration experiment, c = 0.077 Ns/m and D = 0.635 J/kg are obtained. Further, by substituting Equations (20), (26) and (27) into Equation (17), the predicted value of the exciting frequency which is most likely to occur is obtained as follows.

$$f_K = \frac{3.2200 \times 2.6292}{4\pi \times 0.077/0.15} \exp\left(-\frac{0.1075}{0.09525}\right) = 0.4244 \text{ Hz}. \tag{30}$$

In order to make the proposed double stable vibration coupling system practical application, the prediction value of the excitation frequency which is most prone to the probability resonance shown in Equation (30) becomes an important factor, and it is necessary to verify the validity of Equation (30) by using the measurement results of actual vibration experiments.

3. Results

For verification, the vibration cases are divided into three cases: excitation of only a random wave signal, excitation of only periodic signals by a small shaker, excitation of both signals at the same time, and the vibration response and vibration generation are measured, respectively. The stochastic resonance phenomenon and the vibration power generation are verified by this experiment. Refer to the prediction Equation (30) of the most likely excitation frequency of probabilistic resonance studied in advance, the frequency of the periodic excitation signal is set to 0.3 Hz to 0.6 Hz, and the amplitude is set to 20 mm uniformly.

The results of the measurement experiment are shown in Figures 7–15. Figures 7a–15a show the results of vibration displacement and vibration generation, wherein the blue line indicates the response vibration displacement of the support table, and the black line indicates the response vibration displacement of the mass block, and the red line indicates the voltage value of the vibration generating power generation. Figures 7b–15b and Figures 7c–15c show vibration displacement velocity diagrams of the support and mass blocks, respectively.

3.1. Vibration by Random Signal

The results of response vibration displacement and vibration power generation obtained when excitation is performed only by random waves are shown in Figure 7. In Figure 7a, when the vibration is oscillated only by random waves, it is possible to confirm that the mass block is always subjected to a single stable vibration in the vicinity of the right equilibrium position because the response vibration displacement is small and the vibrator starts from the right equilibrium position. When the amplitude of the response vibration displacement is small, the voltage of the oscillatory power generation by the piezoelectric element is small, the average voltage value is 1.75 V, and the maximum voltage value is

6.70 V. It is understood that the difference between the vibration displacement amplitudes of the support base and the mass block is not large by comparing the values shown in Figure 7b,c, and the maximum speed of the mass block is larger than the support table.

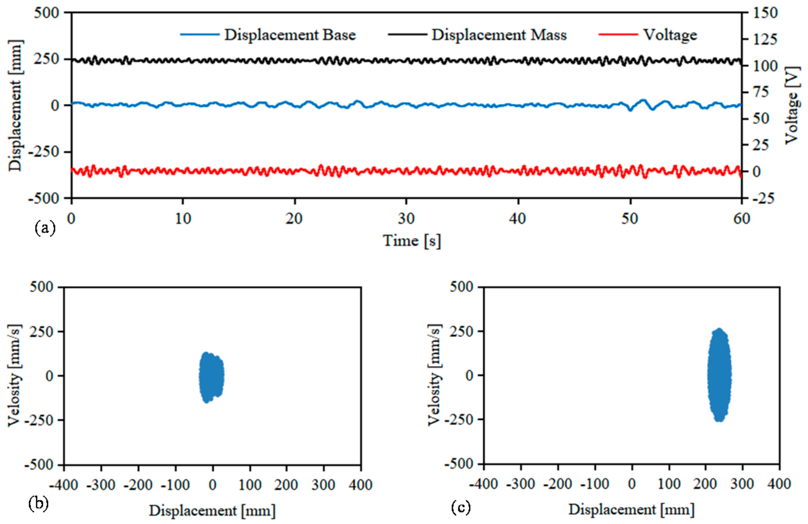

Figure 7. Measurement results of response vibration displacement and vibration power generation when vibrating with a random signal. (**a**) Results of response vibration displacement. (**b**) Diagram of displacement velocity of vibration of the support. (**c**) Diagram of displacement velocity of vibration of the mass block.

3.2. Vibration by Period Signal

The results of response vibration displacement and vibration power generation obtained when the signal is vibrated with a periodic signal by a mini shaker are shown in Figures 8–11.

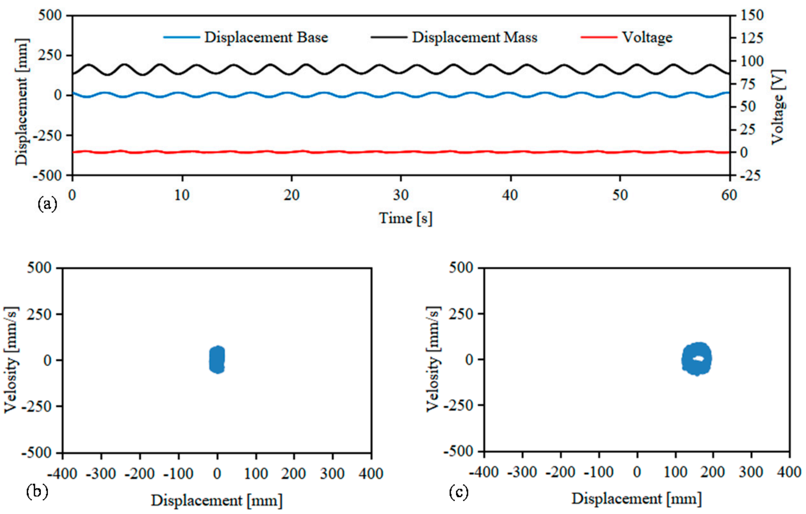

Figure 8. Measurement results of response vibration displacement and vibration power generation when vibrating with a period signal 0.3 Hz. (**a**) Results of response vibration displacement. (**b**) Diagram of displacement velocity of vibration of the support. (**c**) Diagram of displacement velocity of vibration of the mass block.

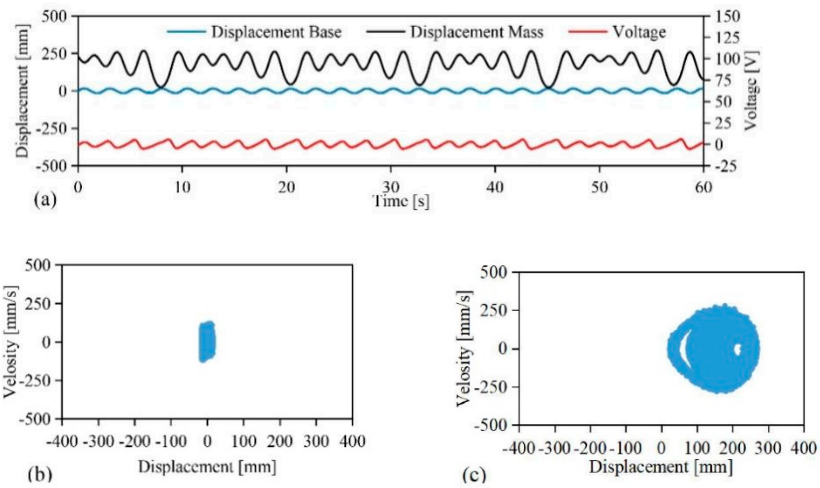

Figure 9. Measurement results of response vibration displacement and vibration power generation when vibrating with a period signal 0.4 Hz. (**a**) Results of response vibration displacement. (**b**) Diagram of displacement velocity of vibration of the support. (**c**) Diagram of displacement velocity of vibration of the mass block.

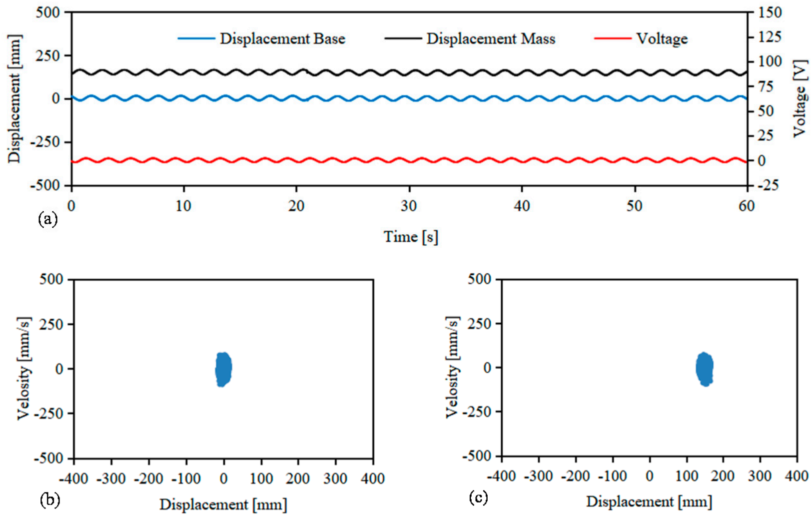

Figure 10. Measurement results of response vibration displacement and vibration power generation when vibrating with a period signal 0.5 Hz. (**a**) Results of response vibration displacement. (**b**) Diagram of displacement velocity of vibration of the support. (**c**) Diagram of displacement velocity of vibration of the mass block.

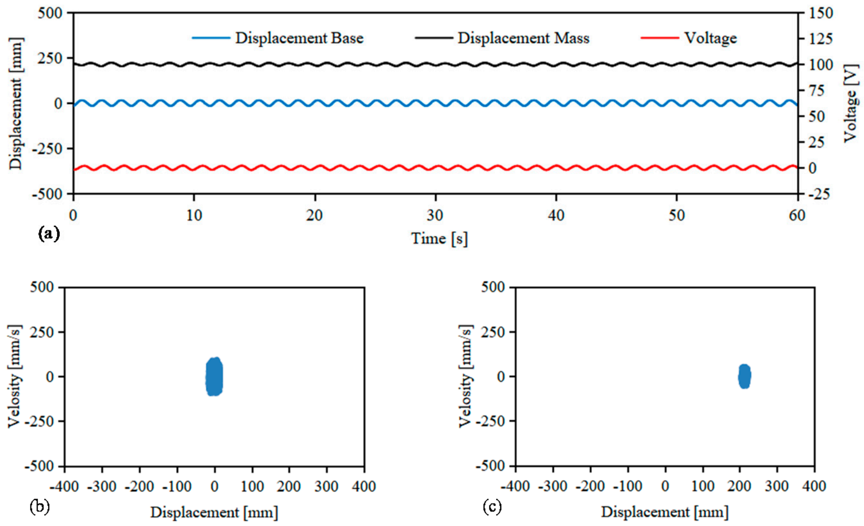

Figure 11. Measurement results of response vibration displacement and vibration power generation when vibrating with a period signal 0.6 Hz. (**a**) Results of response vibration displacement. (**b**) Diagram of displacement velocity of vibration of the support. (**c**) Diagram of displacement velocity of vibration of the mass block.

As shown in Figure 8, the response vibration of the mass block oscillates at the same frequency as the support table, and the response vibration displacement of the mass block is a little larger than the support stage, and the vibration of the mass block becomes a little larger than the support stage, and it makes the single steady vibration on the right side of the vibration model can be confirmed. In addition, since the relative motion of the mass block and the support table is small, the voltage of the oscillatory power generation by the piezoelectric element is small, the average voltage value is 0.44 V, and the maximum voltage value is 1.26 V. Figure 8a,b show that the vibration displacement and the speed of the mass block are relatively small.

Figure 9 shows a measurement result obtained by the excitation of a periodic signal of 0.4 Hz frequency, it was found that the vibration was clearly more extensive than the vibration displacement at 0.3 Hz. Moreover, the vibration of the periodic response vibration displacement is slightly disturbed, and it is considered that the vibration frequency is likely to approach the natural frequency of the vibration model. However, the response vibration of the mass block remains on the right side of the vibration model, and it is confirmed that a single stable vibration is performed. In addition, since the relative motion of the mass block and the support table became relatively large, the voltage of the oscillatory power generation by the piezoelectric element became a little larger, and the average voltage value was 2.84 V, and the maximum voltage value was 6.86 V. The vibration displacement and the velocity of the mass block are clearly increased by Figure 9a,b, and the vibration is continued to the vibration model's right side.

Figures 10 and 11 show the results of measurement in the case where the signal is oscillated with a periodic signal having a frequency of 0.5 Hz and 0.6 Hz, it was found that the vibration displacement was clearly reduced compared with the vibration displacement at 0.4 Hz. In addition, since the relative motion of the mass block and the support table became small, the voltage of the oscillatory power generation by the piezoelectric element became small, the average voltage value at the frequency of 0.5 Hz was 1.29 V, the maximum voltage value was 2.14 V, the average voltage value at the frequency of 0.6 Hz was 1.28 V, and the maximum voltage value was 2.27 V. And, the vibration displacement and the velocity of the mass block are clearly reduced by the relation graph of the response vibration displacement and the speed, and the vibration is continued to the right side of the vibration model.

3.3. Vibration by Random and Period Signal

Figures 12–15 show the results of response vibration displacement and vibration power generation obtained in the joint excitation with random wave signals and periodic signals by mini shaker.

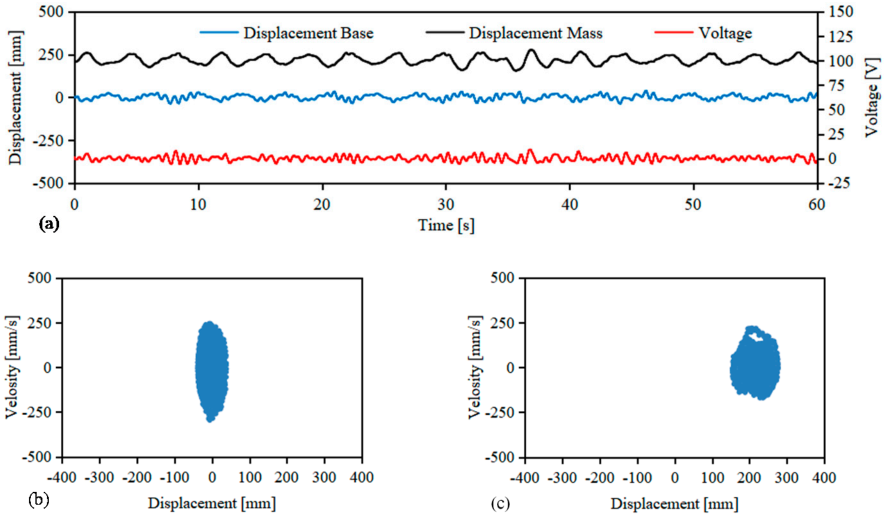

Figure 12. Measurement results of response vibration displacement and vibration power generation when vibrating with a random signal and a period signal 0.3 Hz. (**a**) Results of response vibration displacement. (**b**) Diagram of displacement velocity of vibration of the support. (**c**) Diagram of displacement velocity of vibration of the mass block.

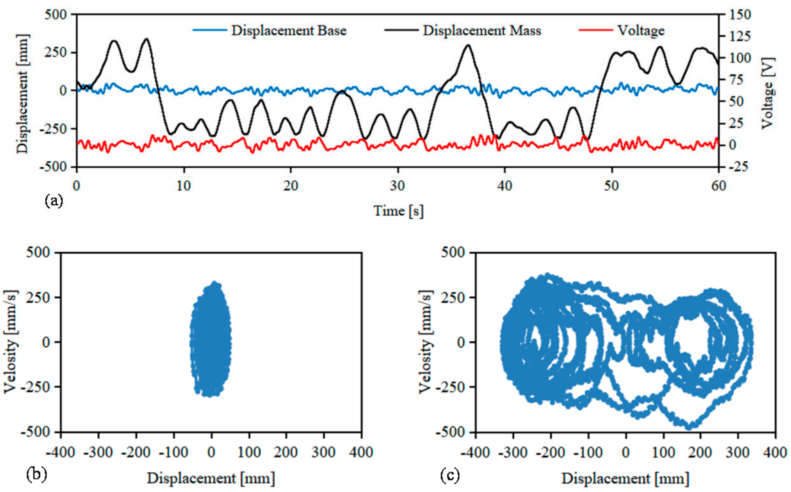

Figure 13. Measurement results of response vibration displacement and vibration power generation when vibrating with a random signal and a period signal 0.4 Hz. (**a**) Results of response vibration displacement. (**b**) Diagram of displacement velocity of vibration of the support. (**c**) Diagram of displacement velocity of vibration of the mass block.

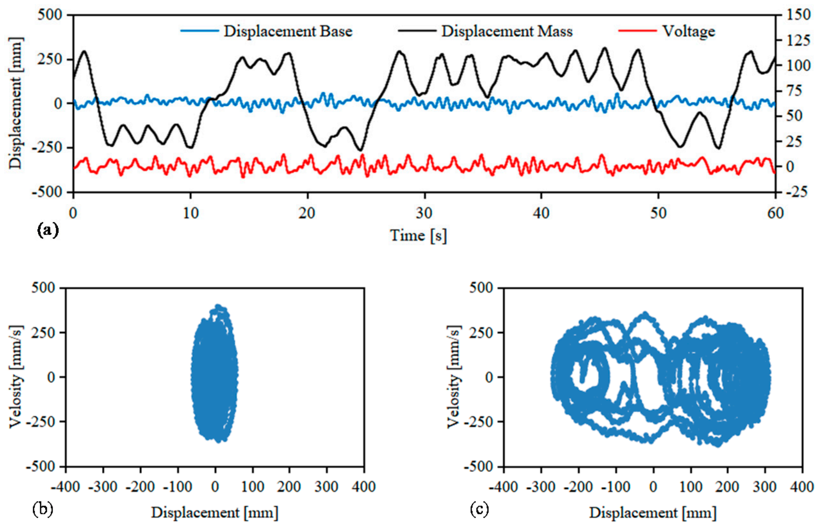

Figure 14. Measurement results of response vibration displacement and vibration power generation when vibrating with a random signal and a period signal 0.5 Hz. (**a**) Results of response vibration displacement. (**b**) Diagram of displacement velocity of vibration of the support. (**c**) Diagram of displacement velocity of vibration of the mass block.

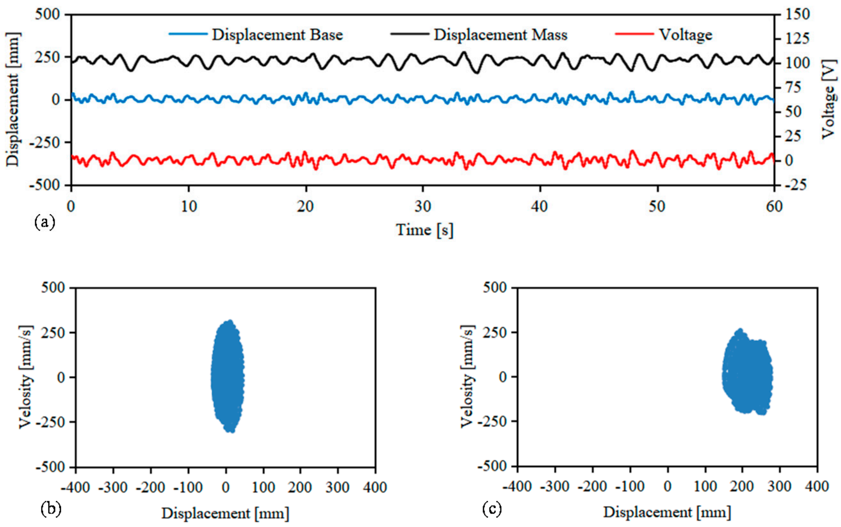

Figure 15. Measurement results of response vibration displacement and vibration power generation when vibrating with a random signal and a period signal 0.6 Hz. (**a**) Results of response vibration displacement. (**b**) Diagram of displacement velocity of vibration of the support. (**c**) Diagram of displacement velocity of vibration of the mass block.

Figure 12 shows the results of the measurement of a random wave signal and a frequency signal of a frequency of 0.3 Hz, the response vibration of the mass block becomes relatively small, and the response vibration displacement of the mass block becomes a random waveform, but it can be confirmed that a single stable vibration is made on the right side of the vibration model. The oscillatory power generation voltage by the piezoelectric element became a little large, and the average voltage value was 1.97 V, and the maximum voltage value was 9.04 V. In Figure 12b,c, the maximum speed of the support table becomes more extensive than the maximum speed of the mass block, and it is confirmed that the single stable vibration is achieved.

Figures 13 and 14 show the results of measurement of a random wave signal and a frequency signal of 0.4 Hz and 0.5 Hz, the response vibration of the mass block becomes intense. It is confirmed that the stochastic resonance phenomenon that makes the bistable vibration crossing both sides beyond the center of the vibration model occurs. As the response vibration becomes intense, the voltage of the oscillatory power generation by the piezoelectric element increases, and the average voltage value at the frequency of 0.4 Hz is 3.29 V, the maximum voltage value is 11.00 V, the average voltage value at the frequency of 0.5 Hz is 3.24 V, and the maximum voltage value is 11.76 V. In addition, the relationship between displacement and velocity shows that the displacement of the mass crosses the two sides of the vibration model and vibrates in a bistable state, which can be understood that stochastic resonance is produced. Figure 15 shows the results of the measurement of a random wave signal and a frequency signal of a frequency of 0.6 Hz.

Figure 15 shows the results of the measurement of a random wave signal and a frequency signal of a frequency of 0.6 Hz; the response vibration of the mass block is reduced again, and the response vibration displacement of the mass block becomes a random waveform, but it can be confirmed that the single steady vibration at the right side of the vibration model is made. In Figure 15b,c, the support table's maximum speed is made a little larger than the maximum speed of the mass block, and it is confirmed that a single stable vibration is achieved.

4. Discussion

4.1. Amplification Effect by Stochastic Resonance

The standard deviation of the response displacement expressed by the following equation can be used to evaluate the magnitude of the response displacement of the vibrator including random vibration.

$$S = \sqrt{\frac{1}{N}\sum_{i=1}^{N}(x_i - \overline{x})^2}. \tag{31}$$

Here, x_i and $\overline{x}$ are measured values of the response displacement, the average value, and N is the sample points of the measurement experiment. In order to evaluate the amplification effect expressed by the ratio of the output and the input of the vibration system, the amplification effect of the proposed bistable vibration model is evaluated using the ratio of the standard deviation of the response displacement of the mass block and the support point calculated in the following equation.

$$S_{ratio} = \frac{S_{mass}}{S_{base}}. \tag{32}$$

Reference numerals S_{mass} and S_{base} denote standard deviation values of the displacement of the mass block and the support point calculated by the Equation (31), respectively. For the measurement result of the vibration experiment shown in Figures 7–15 discussed in the previous section, S_{ratio} is calculated in Equation (32), and the result is summarized in Figure 16.

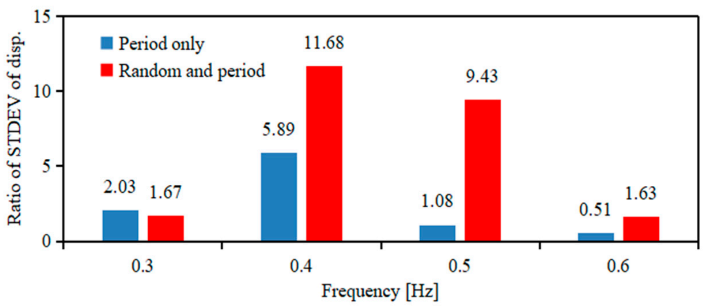

Figure 16. Results of comparing Ratio of displacement standard deviation of mass block to support point. (The blue graph is the result of vibration with a periodic signal. The red graph is the result of vibration with random and periodic signals).

In Figure 16, the blue graph shows S_{ratio} when the periodic signal is vibrated, and the red graph shows S_{ratio} when the random signal is combined with the periodic signal. As shown in Figure 16, in the case where the random signal is combined with the periodic signals of 0.4 Hz and 0.5 Hz, a stochastic resonance of bistable oscillation occurs, it is confirmed that the obtained amplification effect can be clearly higher than the other single stable motion states.

For further comparison, the sum of an excited by random signal and periodic signal S_{ratio} is 1.06 + 5.89 = 6.95, and an excited by common signal S_{ratio} is 11.68, the difference is 68.06%. In the case of the periodic signal of 0.5 Hz, the sum of the obtained sum S_{ratio} was 1.06 + 1.08 = 2.14, and the joint vibration S_{ratio} was 9.43, and the difference between them was 340.65%. It was confirmed that both of them were higher than the sum obtained by excitation. This seems to be due to the stochastic resonance.

4.2. Efficiency Evaluation of Vibration Power Generation

The average electric power represented by the following equation is used to evaluate the power generation of a bistable vibration harvesting system.

$$W_{aver} = \frac{1}{T}\int \frac{V^2}{R}dt = \frac{1}{NR}\sum_{i=1}^{N} V_i^2. \tag{33}$$

Here, V and V_i are measured values of voltage and voltage measurements, R is load resistance load resistance, and T and N are measured sample time and sample points of excitation experiment, respectively. In this study, $R = 1$ KΩ, T = 60 s, N = 10,000.

Here, W_{aver} is calculated in Equation (33) for the measurement result of the vibration experiment shown in Figures 7–15 which are considered in the previous section, and the result is summarized in Figure 17.

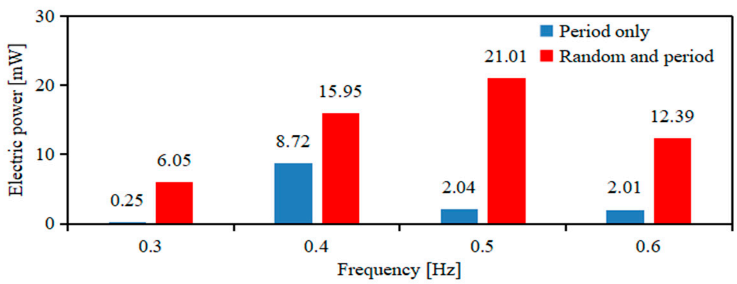

Figure 17. Results of comparing average electrical power. (The blue graph is the result of vibration with a periodic signal. The red graph is the result of vibration with random and periodic signals).

In Figure 17, the blue graph shows W_{aver} when the periodic signal is vibrated, and the red graph shows W_{aver} when the random signal is combined with the periodic signal. As shown in Figure 17, when the frequency of the periodic signal increases, the generation of the power generation tends to increase, but, in the case of the joint vibration with the random signal and the periodic signal of 0.4 Hz and 0.5 Hz, the stochastic resonance of bistable vibration is generated, and it can be confirmed that the obtained W_{aver} is higher than other single stable motion states.

For more detailed comparison, the result obtained by adding the Waver obtained by the excitation of the random signal and the periodic signal separately, when compared with the Waver, in the case of the periodic signal of 0.4 Hz, the sum of the waves obtained by the separate excitation was 4.72 + 8.72 = 13.44 mW, and the vibration was 15.95 mW, and the difference between them was 18.68%.

In the case of the periodic signal of 0.5 Hz, the sum of the waves obtained by the separate excitation was 4.72 + 2.04 = 6.76 mW, and the joint vibration was 21.01 mW, and the difference between them was 210.80%.

4.3. Effect of Amplitude of Periodic Excitation Signal

In order to generate the stochastic resonance, it is necessary to vibrate with the periodic signal by the mini shaker, however, periodic excitation signals exist in nature and do not necessarily have to be artificially shown in the research results of the literature. In order to investigate the effect of frequency and amplitude on the initial stage of the study, this paper has given a periodic excitation signal using a mini shaker.

In the previous section, the effect of the frequency of the periodic excitation signal on the stochastic excitation was examined by the measurement experiment; here, in order to examine the effect of the amplitude of the periodic excitation signal, the response vibration of the mass block is set to 0.45 Hz from the most intense frequency, the amplitude is set to 15 mm, 20 mm, and 25 mm, respectively, and the excitation experiment is performed; the measured results are shown in Figures 18–20.

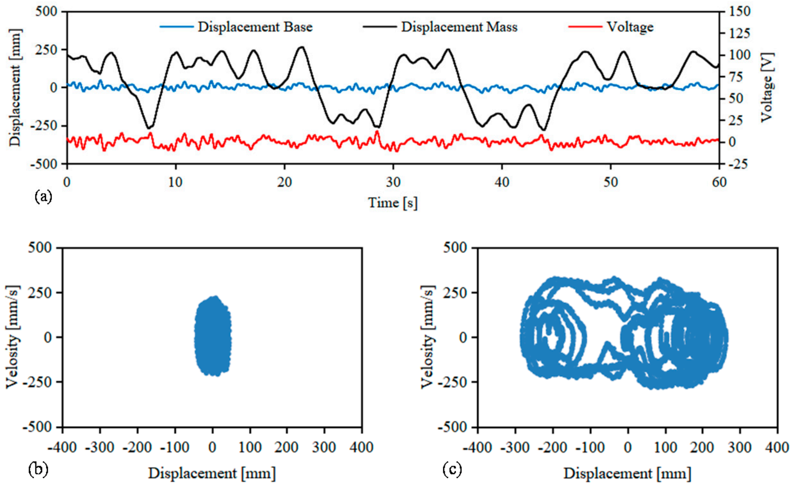

Figure 18. Measurement results of response vibration displacement and vibration power generation when vibrating with a random signal and a period signal 0.45 Hz of small amplitude 15 mm. (**a**) Results of response vibration displacement. (**b**) Diagram of displacement velocity of vibration of the support. (**c**) Diagram of displacement velocity of vibration of the mass block.

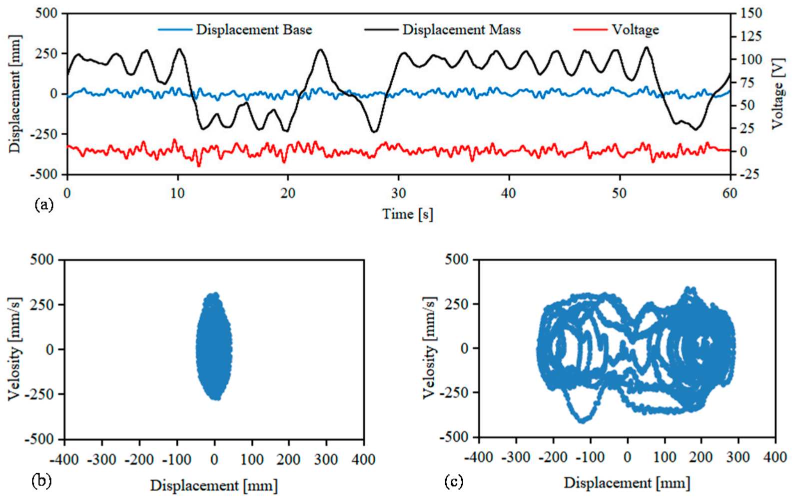

Figure 19. Measurement results of response vibration displacement and vibration power generation when vibrating with a random signal and a period signal 0.45 Hz of middle amplitude 20 mm. (**a**) Results of response vibration displacement. (**b**) Diagram of displacement velocity of vibration of the support. (**c**) Diagram of displacement velocity of vibration of the mass block.

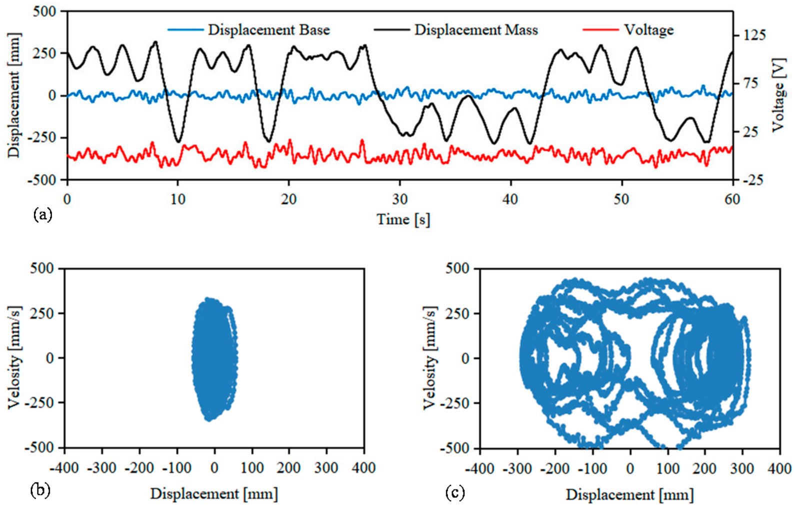

Figure 20. Measurement results of response vibration displacement and vibration power generation when vibrating with a random signal and a period signal 0.45 Hz of large amplitude 25 mm. (**a**) Results of response vibration displacement. (**b**) Diagram of displacement velocity of vibration of the support. (**c**) Diagram of displacement velocity of vibration of the mass block.

In the figure, if the excitation frequency is set correctly, regardless of the amplitude, the resonant resonance is generated in the case of three amplitude excitation. The correlation between response vibration displacement and velocity graph is compared, when the amplitude of the periodic excitation signal is different, the maximum speed of the response vibration of the support stage tends to be a little larger, and the maximum speed of the response vibration of the mass block also becomes larger as the amplitude increases. Moreover, in the three excitation cases, the response vibration of the mass block clearly shows the bistable vibration across both sides of the vibration model, and the stochastic resonance phenomenon is generated.

However, it can be confirmed that the voltage value of the generated vibration power generation is changed slightly by the difference in the amplitude of the periodic excitation signal. The average voltage value at a small amplitude of 15 mm is 3.27 V, the maximum voltage value is 12.19 V, the average voltage value at the middle amplitude of 20 mm is 3.28 V, the maximum voltage value is 16.63 V, the average voltage value at 25 mm of the large amplitude is 4.17 V, and the maximum voltage value is 16.29 V.

The results of calculating the average electric power are summarized in Figure 21. As shown in Figure 21, by increasing the amplitude of the periodic excitation signal, the average electric power obtained can be confirmed to be a little larger. Therefore, it is possible to confirm that the amplification effect which changes from the single stable vibration state to the bistable vibration state is large, and that the vibration generation quantity using the amplification effect is larger than the pursuit of the vibration generation quantity by simply increasing the vibration amplitude.

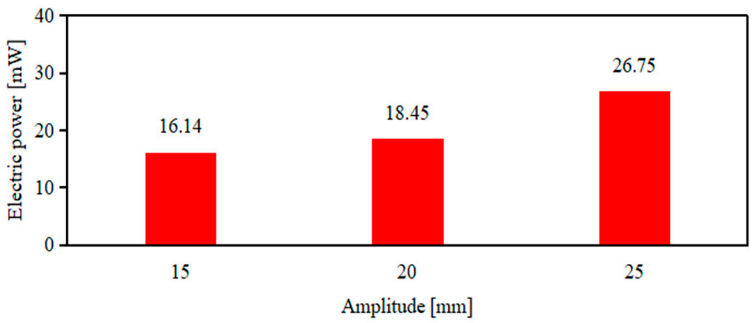

Figure 21. Results of comparing average electrical power with different amplitude.

4.4. Applicable Conditions for Vibration Power Generation

An inverted cantilever beam bistable model was used in this study. When a cantilever beam with a mass block at its tip is in a stationary state, the cantilever beam is bent laterally by the gravity of the mass block, the position is stopped at the position as shown in Figure 22, and the position becomes the vibration center point of the single stable vibration. In addition, since the vibration model is a left-right symmetrical structure, and there is a single stable vibration state on both sides of the central symmetry axis, it is easy to judge that the model can form a double stable vibration system.

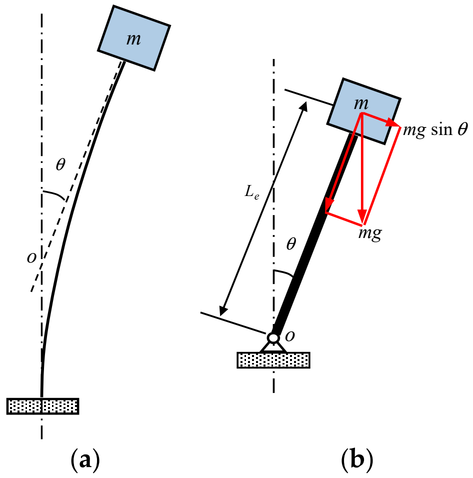

Figure 22. Bi-stable vibration model of inverted cantilever with lumped mass block at its tip. (**a**) Original vibration model. (**b**) Virtual vibration model.

When the mass of the mass block of Figure 22 is relatively small, the cantilever beam in the stationary state moves along the vertical direction. The mass block stops at the symmetry axis position, and the vibration model becomes a single stable vibration centered on the symmetry axis. In other words, it is necessary to consider the conditions necessary for the bistable oscillation. According to Reference [38], maximum deflection equation for lateral loading of cantilever beams subjected to lateral loading, as follows:

$$\delta = \frac{PL^3}{3EI}. \tag{34}$$

From Equation (34), bending stiffness of cantilever beams can be calculated by the following equation:

$$K_{Beam} = \frac{P}{\delta} = \frac{3EI}{L^3}. \tag{35}$$

In the equation, K_{beam} is the flexural rigidity of the cantilever beam, L is the length of the beam, E is the elastic Young's modulus of the material, and I is the second moment of the beam.

According to Reference [38], the angle of inclination of the center point of the mass block can be calculated by the following equation.

$$\theta = \frac{PL^2}{2EI}. \tag{36}$$

The distance from the center point to the intersection point O of the concentrated mass block is expressed by the following, Equations (34) and (35):

$$L_e = \frac{\delta}{\theta} = \frac{2L}{3}. \tag{37}$$

By Equation (37), in the course of vibration, since the distance Le is always constant in relation to the length L of the beam, it is possible to apply the virtual model to the virtual model of the rigid link with the mass block at the tip of Figure 22b, and to consider the vibration characteristic using the virtual model. In the equivalent model shown in Figure 22b, the bending rigidity K_{Mass} for deformation of the mass block by gravity mg and returning it to the center symmetry axis is approximately expressed by the following equation.

$$K_{Mass} = \frac{mg \sin\theta}{L_e \theta} = \frac{mg}{L_e}. \tag{38}$$

Equation (37) is substituted for Equation (38) to obtain the following equation:

$$K_{Mass} = \frac{3mg}{2L}. \tag{39}$$

By comparing the Equations (35) and (39), if $K_{Beam} > K_{Mass}$, the cantilever beam is kept in the vertical position in the stationary state because of its strong flexural rigidity, the vibration of a mass block becomes a single stable vibration centering on the symmetry axis. Conversely, if $K_{Mass} \geq K_{Beam}$, the equation can be obtained by Equations (35) and (39), as follows:

$$mg \geq \frac{2EI}{L^2}. \tag{40}$$

Since the cantilever beam's flexural rigidity is relatively weak, the cantilever beam is bent laterally by the gravity of the mass block, and the mass block is initially displaced. The vibration state is bistable vibration centered on the two initial displacement positions on the left and right sides. Therefore, it can be seen from Equation (40) that the vibration state of the inverted cantilever beam vibration model with mass block at the front end is a necessary condition for the double stable vibration.

In order to further examine, the equation for calculating the limit load for the cantilever beam subjected to compressive pressure in the axial direction and yielding the Euler buckling is expressed as follows [38]:

$$P_{cr} = \frac{\pi^2 EI}{4L^2} = \frac{2.465EI}{L^2}. \tag{41}$$

In order to maintain a stable vibration state, it is desirable to oscillate in a range where no buckling occurs, and the following equation is obtained, taking into account the Equations (40) and (41).

$$\frac{2EI}{L^2} < mg < \frac{2.465EI}{L^2}. \tag{42}$$

The design range of the bistable vibration model of the inverted cantilever beam of this study shown in Figure 22 is represented by Equation (42).

5. Conclusions

In this study, in order to develop renewable energy, a vibration power generation system using a bistable vibration model for an inverted cantilever beam is designed, and the following conclusions were obtained.

1. The stochastic resonance phenomenon by the bistable oscillation model in the random wave environment can be reproduced in the laboratory, and theoretical analysis shows that the vibration system has bistable vibration characteristics in the wide range of displacement. In addition, by using Kramer rate, the prediction equation of the excitation frequency of the proposed bistable vibration model is obtained.
2. Using the experimental apparatus developed in this experiment, we can confirm the stochastic resonance which changes the response from mass stability to bistable vibration, the amplification effect was evaluated quantitatively by the measurement results. As a result of the actual measurement, the frequency range in which the

probability resonance is most likely to be generated is 0.4 Hz to 0.5 Hz, and this measurement result coincides with the theoretical prediction value of 0.42 Hz in this research.

3. We have developed a bistable vibratory power generation system using piezoelectric elements, a case in which stochastic resonance does not occur; average electric workability was measured by vibration generated, and the measurement results confirmed the effectiveness of the stochastic resonance.
4. Our practical application of a vibratory power generation system to a random wave environment using bistable vibration model was performed; the study on bistable vibration model of an inverted cantilever beam with a mass block at its tip, providing design coverage for detailed configuration parameters, the basic technology which is useful for the research and development of the vibration power generation system for future renewable energy development was prepared.

Author Contributions: Q.W. contributed to study concepts, study design and manuscript preparation; H.Z., J.L. and S.Z. contributed to data acquisition and manuscript editing; W.Z. and X.Z. contributed to guarantor of integrity of entire study. All authors have read and agreed to the published version of the manuscript.

Funding: This research received no external funding.

Institutional Review Board Statement: Not applicable.

Informed Consent Statement: Not applicable.

Data Availability Statement: Data available in a publicly accessible repository.

Conflicts of Interest: The authors declare no conflict of interest.

References

1. Mohanty, A.; Parida, S.; Behera, R.K.; Roy, T. Vibration energy harvesting: A review. *J. Adv. Dielectr.* **2019**, *9*, 17. [CrossRef]
2. Zhang, H.; Corr, L.R.; Ma, T. Issues in vibration energy harvesting. *J. Sound Vib.* **2018**, *421*, 79–90. [CrossRef]
3. Hadas, Z.; Singule, V. Energy Harvesting—Opportunity for Future Remote Applications. In Proceedings of the 17th International Conference Engineering Mechanics, Svratka, Czech Republic, 9–12 May 2011.
4. Stephen, N.G. On energy harvesting from ambient vibration. *J. Sound Vib.* **2006**, *293*, 409–425. [CrossRef]
5. Moss, S.D.; Payne, O.R.; Hart, G.A.; Ung, C. An Investigation on Physical Limitations in Vibration Energy Harvesting. *Smart Mater. Struct.* **2015**, *24*, 023001. [CrossRef]
6. Tang, L.; Yang, Y.; Soh, C.K. Toward Broadband Vibration-based Energy Harvesting. *J. Intell. Mater. Syst. Struct.* **2010**, *21*, 1867–1897. [CrossRef]
7. Benzi, R.; Sutera, A.; Vulpiani, A. The mechanism of stochastic resonance. *J. Phys. A Math. Gen.* **1981**, *14*, 453–457. [CrossRef]
8. Gammaitoni, L.; Hänggi, P.; Jung, P.; Marchesoni, F. Stochastic resonance. *Rev. Mod. Phys.* **1999**, *70*, 223–287. [CrossRef]
9. McNamara, B.; Wiesenfeld, K. Theory of stochastic resonance. *Phys. Rev. A* **1989**, *39*, 4854–4869. [CrossRef]
10. Tretyakov, M.V. Numerical technique for studying stochastic resonance. *Phys. Rev. E* **1998**, *57*, 4789–4794. [CrossRef]
11. Jiang, W.-A.; Chen, L.-Q. Stochastic averaging of energy harvesting systems. *Int. J. Non-Linear Mech.* **2016**, *85*, 174–187. [CrossRef]
12. Lin, R.; Ng, T.Y.; Fan, Z. New Type of Spectral Nonlinear Resonance Enhances Identification of Weak Signals. *Sci. Rep.* **2019**, *9*, 14125. [CrossRef]
13. Jung, P.; Hänggi, P. Amplification of small signals via stochastic resonance. *Phys. Rev. A* **1991**, *44*, 8032–8042. [CrossRef] [PubMed]
14. Zhang, Z.; Ma, J. Adaptive parameter-tuning stochastic resonance based on SVD and its application in weak IF digital signal enhancement. *J. Adv. Signal Process.* **2019**, *2019*, 24. [CrossRef]
15. Krauss, P.; Metzner, C.; Schilling, A.; Schütz, C.; Tziridis, K.; Fabry, B.; Schulze, H. Adaptive stochastic resonance for unknown and variable input signals. *Sci. Rep.* **2017**, *7*, 2450. [CrossRef]
16. Ghosh, P.K.; Marchesoni, F.; Savel'Ev, S.E.; Nori, F. Geometric Stochastic Resonance. *Phys. Rev. Lett.* **2010**, *104*, 020601. [CrossRef]
17. Jha, R.K.; Biswas, P.K.; Chatterji, B.N. Image Denoising using Stochastic Resonance. In Proceedings of the International Conference on Cognition and Recognition; 2014; pp. 343–348.
18. Marks, R.J.; Thompson, B.; El-Sharkawi, M.; Fox, W.; Miyamoto, R. Stochastic resonance of a threshold detector: Image visualization and explanation. In Proceedings of the 2002 IEEE International Symposium on Circuits and Systems (ISCAS), Phoenix-Scottsdale, AZ, USA, 26–29 May 2002; Volume 4, pp. 521–523.
19. Simonotto, E.; Riani, M.; Seife, C.; Roberts, M.; Twitty, J.; Moss, F. Visual Perception of Stochastic Resonance. *Phys. Rev. Lett.* **1997**, *78*, 1186–1189. [CrossRef]
20. Harne, R.L.; Wang, K.W. A review of the recent research on vibration energy harvesting via bistable systems. *Smart Mater. Struct.* **2013**, *22*, 023001. [CrossRef]

21. Pellegrini, S.P.; Tolou, N.; Schenk, M.; Herder, J.L. Bistable vibration energy harvesters: A review. *J. Intell. Mater. Syst. Struct.* **2012**, *24*, 1303–1312. [CrossRef]
22. Baltanás, J.P.; López, L.; Blechman, I.I.; Landa, P.S.; Zaikin, A.; Kurths, J.; Sanjuán, M.A.F. Experimental evidence, numerics, and theory of vibrational resonance in bistable systems. *Phys. Rev. E* **2003**, *67*, 066119. [CrossRef]
23. Yao, C.; Liu, Y.; Zhan, M. Frequency-resonance-enhanced vibrational resonance in bistable systems. *Phys. Rev. E* **2011**, *83*, 061122. [CrossRef] [PubMed]
24. Zheng, R.; Nakano, K.; Hu, H.; Su, D.; Cartmell, M.P. An application of stochastic resonance for energy harvesting in a bistable vibrating system. *J. Sound Vib.* **2014**, *333*, 2568–2587. [CrossRef]
25. Nakano, K.; Cartmell, M.P.; Hu, H.; Zheng, R. Feasibility of Energy Harvesting Using Stochastic Resonance Caused by Axial Periodic Force. *J. Mech. Eng.* **2014**, *60*, 314–320. [CrossRef]
26. Wang, K.; Dai, X.; Xiang, X.; Ding, G.; Zhao, X. Optimal potential well for maximizing performance of bi-stable energy harvester. *Appl. Phys. Lett.* **2019**, *115*, 143904. [CrossRef]
27. Ibrahim, A.; Towfighian, S.; Younis, M.I. Dynamics of Transition Regime in Bi-stable Vibration Energy Harvesters. *J. Vib. Acoust.* **2017**, *139*, 051008. [CrossRef]
28. Leng, Y.G.; Gao, Y.J.; Tan, D.; Fan, S.B.; Lai, Z.H. An elastic-support model for enhanced bistable piezoelectric energy harvesting from random vibrations. *J. Appl. Phys.* **2015**, *117*, 064901. [CrossRef]
29. Bilgen, O.; Ali, S.F.; Friswell, M.I.; Litak, G.; De Angelis, M. Non-linear piezoelectric vibration energy harvesting from a vertical cantilever beam with tip mass. *J. Intell. Mater. Syst. Struct.* **2012**, *23*, 1505–1521. [CrossRef]
30. Bilgen, O.; Friswell, M.I.; Ali, S.F.; Litak, G. Broadband Vibration Energy Harvesting from a Vertical Cantilever Piezocomposite Beam with Tip Mass. *Int. J. Struct. Stab. Dyn.* **2015**, *15*, 1450038. [CrossRef]
31. Lan, C.; Qin, W.Y. Energy harvesting from coherent resonance of horizontal vibration of beam excited by vertical base motion. *Appl. Phys. Lett.* **2014**, *105*, 113901. [CrossRef]
32. Cleante, V.G.; Brennan, M.J.; Gatti, G.; Thompson, D.J. On the target frequency for harvesting energy from track vibrations due to pass ing trains. *Mech. Syst. Signal Process.* **2019**, *114*, 212–223. [CrossRef]
33. Qiang, F.; Xu, T.B.; Zhao, L. Piezoelectric energy harvesting from human walking using a twostage amplification mechanism. *Energy* **2019**, *189*, 116140. [CrossRef]
34. Rodrigues, C.; Ramos, M.; Esteves, R.; Correia, J.; Clemente, D.; Gonçalves, F.; Mathias, N.; Gomes, M.; Silva, J.; Duarte, C.; et al. Integrated study of triboelectric nanogenerator for ocean wave energy harvesting: Performance assessment in realistic sea conditions. *Nano Energy* **2021**, *84*, 105890. [CrossRef]
35. Chen, Y.S.; Gu, C.; Zhao, P.; Chen, W. Research on Piezoelectric Energy harvesting from Multi-Direction Wind-Induced Vibrations. *IOP Conf. Ser. Earth Environ. Sci.* **2020**, *617*, 012014. [CrossRef]
36. Zhang, Y.; Zheng, R.; Ejiri, K.; Su, D.; Nakano, K. Modelling analysis for vibration energy harvesting excited by low-speed automobile tires. *Trans. JSME* **2016**, *842*, 840. (In Japanese) [CrossRef]
37. Zhang, Y.; Zheng, R.; Kaizuka, T.; Su, D.; Nakano, K.; Cartmell, M. Broadband vibration energy harvesting by application of stochastic resonance from rotational environments. *Eur. Phys. J. Spec. Top.* **2015**, *224*, 2687–2701. [CrossRef]
38. Beer, F.P.; Johnston, E.R.; Dewolf, J.T.; Mazurek, D.F. *Mechanics of Materials*; McGraw-Hill: New York, NY, USA, 2012.